

Vacuum Birefringence in a Supercritical Magnetic Field and a Subcritical Electric Field

Chul Min Kim*

*Center for Relativistic Laser Science, Institute for Basic Science, Gwangju 61005, Korea and
Advanced Photonics Research Institute, Gwangju Institute of Science and Technology, Gwangju 61005, Korea*

Sang Pyo Kim†

Department of Physics, Kunsan National University, Kunsan 54150, Korea

(Dated: February 14, 2022)

Recent ultra-intense lasers of subcritical fields and proposed observations of the x-rays polarization from highly magnetized neutron stars of supercritical fields have attracted attention to vacuum birefringence, a unique feature of nonlinear electrodynamics. We propose a formulation of vacuum birefringence that incorporates the effects of the weaker electric field added to the extremely strong magnetic field. To do so, we first derive a closed analytical expression for the one-loop effective Lagrangian for the combined magnetic and electric fields by using an explicit formula of the one-loop effective Lagrangian for an arbitrarily strong magnetic field. We then employ the expression to derive the polarization and magnetization of the vacuum, from which the permittivity and permeability for weak probe fields are obtained. Finally, we find the refractive indices and the associated polarization vectors for the case of parallel magnetic and electric fields. The proposed formulation predicts that an electric field along the magnetic field reduces the birefringence and rotates the polarization vectors. Such effects should be taken into account for accurate polarimetry of the x-rays from magnetized neutron stars, which will prove the fundamental aspect of the strong field quantum electrodynamics (QED) and explore the extreme fields of astrophysical bodies.

Keywords: vacuum birefringence, photon-photon scattering, effective Lagrangian, electromagnetic wrench, neutron star

I. INTRODUCTION

A background electromagnetic field polarizes the Dirac vacuum and produces charged particles-antiparticle pairs. Heisenberg-Euler and Weisskopf found the one-loop effective Lagrangian in a constant electromagnetic field [1, 2], and Schwinger obtained the effective Lagrangian in the proper-time integral by integrating out the fermion or scalar boson coupled to the electromagnetic field within quantum electrodynamics (QED) [3]. The imaginary part of the proper-time integral, contributed by simple poles, gives the loss of the vacuum persistence due to pair production. In fact, a pure electric field or electric field parallel to a magnetic field in a proper Lorentz frame produces electron-positron pairs from the Dirac sea via quantum tunneling through the tilted mass gap. The correct electromagnetic theory should be described by the effective action consisting of the Maxwell action and the loop corrections due to strong electromagnetic fields. Hence, a probe photon propagates through a polarized vacuum due to the effective action, and prominent phenomena of vacuum polarization can occur such as vacuum birefringence, photon splitting, photon-photon scattering, etc [4].

The pair production, called the Schwinger effect, is a nonperturbative effect of quantum field theory. The electron-positron pairs can be efficiently produced when the electric field is comparable to the critical field $E_{\text{cr}} = m^2 c^3 / e \hbar = 1.3 \times 10^{16}$ V/cm since the pair production rate per a unit four Compton volume is given by the Boltzmann factor of which exponent is given as the negative of the ratio of the critical field to the electric field. The magnetic field of the critical strength, $B_{\text{cr}} = m^2 c^3 / e \hbar = 4.4 \times 10^{13}$ G, makes the lowest Landau energy equal to the rest mass of the electron. The critical strengths E_{cr} and B_{cr} are called the Schwinger fields. The effect of vacuum polarization and the Schwinger pair production can be measured when the electromagnetic fields are comparable to or higher than the critical field. Thus, the physics in strong electromagnetic fields that is governed by the effective action drastically differs from the physics in weak fields that obeys the Maxwell theory.

In experiments, the Schwinger pair production is still very difficult to realize because no terrestrial mean provides an electric field comparable to the Schwinger field. In spite of the recent progress in high-intensity lasers based on chirped pulsed amplification (CPA) technique, the current highest laser intensity is 1.1×10^{23} W/cm², achieved by

* chulmin@gist.ac.kr

† sangkim@kunsan.ac.kr

CoReLS [5], of which field strength is still lower than the critical field by three orders. Several laser facilities are being constructed for higher intensities, but the target fields strengths are still lower by order one or two [6].

In contrast, the effects of vacuum polarization such as photon-photon scattering have been experimentally investigated. The Delbrück scattering, in which a photon is scattered by a Coulomb field, was observed with MeV photons [7, 8]. The photon splitting, in which a photon is split into two by a Coulomb field was also observed [9]. These observations were enabled by the strong nuclear Coulomb field. The photon-photon scattering without a Coulomb field is more difficult to realize but was recently evidenced from heavy ion collision experiments: the ATLAS experiment [10, 11] and the CMS experiment [12].

The photon-photon scattering can also occur under a magnetic field. The Delbrück scattering by a magnetic field leads to the vacuum birefringence, and, as a consequence, the vacuum under a strong magnetic field can act as a birefringent medium to low-energy photons. Compared to the Schwinger pair production and the photon-photon scattering by the nuclear Coulomb field, the vacuum birefringence has the advantage of accumulating the effect over a macroscopic length scale. To realize the vacuum birefringence, the PVLAS project uses the magnetic field from a strong permanent magnet as the background field and optical laser photons as the probe photons [13]. Also, it was proposed to use the field from an ultra-intense laser as the background field and the strong x-rays from an x-ray free electron laser as the probe photons [14, 15]. This proposal relies on the state-of-arts scientific technologies such as ultra-intense lasers [6], x-ray free electron lasers [16], and ultra-high-precision x-ray polarimetry [17]. Albeit challenging, the goal of the PVLAS project and the laser-based proposal is limited to the vacuum birefringence in subcritical fields.

On the other hand, highly magnetized neutron stars have magnetic fields comparable to the critical field, and particularly magnetars have magnetic fields stronger than the critical field [18–20]. The dipole model for pulsars and highly magnetized neutron stars provides strong dipole magnetic fields and weak induced electric fields [21]. Therefore, it will be interesting to study the QED vacuum polarization effect in such supercritical magnetic fields and subcritical electric fields, which can provide a diagnostics for strong electromagnetic fields of neutron stars [22]. Recently, the observation of the x-rays from highly magnetized neutron stars by using space telescopes has been proposed [23, 24]. Furthermore, the scale of field variation is the radius of the neutron star so that the one-loop effective action can be accurately given by the Heisenberg-Euler and Schwinger action.

To explicitly express the vacuum birefringence in supercritical magnetic fields, a closed analytic expression of one-loop effective action is more convenient than the proper-time integral expression obtained by Heisenberg-Euler and Schwinger. Dittrich employed the dimensional regularization method to perform the proper-time integral in terms of the Hurwitz zeta-function and logarithmic functions in either a pure magnetic field or an electric field perpendicular to the magnetic field [25, 26]. In Ref. [27], the in-out formalism that leads to the proper-time integral also directly gives the closed analytic expression for the one-loop effective Lagrangian in the same field configuration, which is identical to the one by Dittrich. Furthermore, the imaginary part of the one-loop Lagrangian in the closed form yields the same result obtained by summing the residues of all simple poles of the proper-time integral [27].

In this paper, we develop the method in [28] to find the closed analytic expression for the one-loop effective action in supercritical magnetic fields combined with subcritical electric fields. Provided that the fields vary little over the Compton length and time, one may use the Heisenberg-Euler and Schwinger one-loop effective Lagrangian in the gauge- and Lorentz-invariant form as a good approximation and can express the one-loop Lagrangian as a power series of a small invariant quantity that becomes the electric field in a Lorentz frame where magnetic and electric fields are parallel to each other. Using the closed expression, we study the propagation modes of a weak probe photon in a vacuum under such electromagnetic fields. For this purpose, we find the permittivity and permeability tensors and obtain the vacuum birefringence for a weak probe photon in parallel electric and magnetic fields.

This paper is organized as follows. In Sec. II, an explicit expression of the one-loop effective Lagrangian is derived for the vacuum under an arbitrarily strong magnetic field superposed with a weaker electric field. The expression is given as a Taylor series in a parameter that is essentially the ratio of the parallel component of the electric field to the magnetic field. Then, in Sec. III, the series is used to obtain the permittivity and permeability tensors for a weak low-frequency probe field. These tensors are used in Sec. IV to find the modes of the probe field (the refractive indices and associated polarization vectors) for the configuration in which the electric field is parallel to the magnetic field. Finally, a conclusion is given, stressing that the presented formulae are necessary to analyze the vacuum birefringence in the pulsar magnetosphere, in which extremely strong magnetic field coexists with a weaker but non-negligible electric field. The Lorentz-Heaviside units with $\hbar = c = 1$ was used, in which the fine structure constant is $\alpha = e^2/4\pi$ (e the elementary charge).

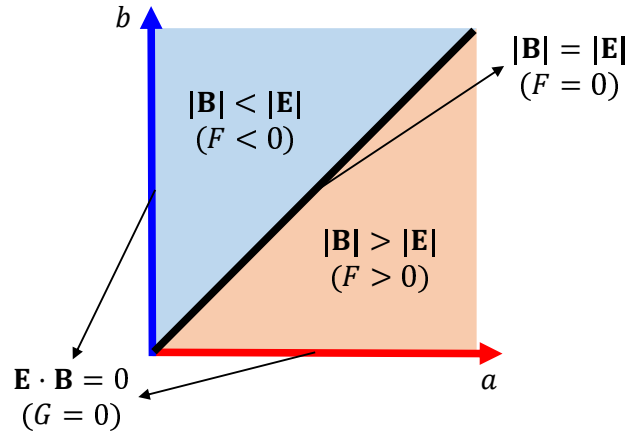


Figure 1. Classification of constant electromagnetic fields in the ab -plane. The diagonal line $b = a$ corresponds to the condition of equally strong electric and magnetic fields, i.e., $|\mathbf{B}| = |\mathbf{E}|$ ($F = (\mathbf{B}^2 - \mathbf{E}^2)/2 = 0$). The horizontal and vertical axes correspond to the wrenchless condition, i.e., $G = -\mathbf{E} \cdot \mathbf{B} = 0$.

II. ONE-LOOP EFFECTIVE LAGRANGIAN OF THE VACUUM UNDER A UNIFORM ELECTROMAGNETIC FIELD

A. Invariant parameters and classification of uniform electromagnetic fields

When dealing with the effective Lagrangian of the vacuum in a constant electromagnetic field, the following Lorentz- and gauge-invariant parameters are convenient for analysis [29]:

$$a = \sqrt{\sqrt{F^2 + G^2} + F}, \quad b = \sqrt{\sqrt{F^2 + G^2} - F}, \quad (1)$$

where $F^{\mu\nu}$ and $F^{*\mu\nu} = \frac{1}{2}\varepsilon^{\mu\nu\alpha\beta}F_{\alpha\beta}$ ($\varepsilon^{0123} = 1$) are the field-strength tensor and its dual, respectively [30]. Then the Maxwell scalar and pseudoscalar are given as

$$F = \frac{1}{4}F^{\mu\nu}F_{\mu\nu} = \frac{1}{2}(\mathbf{B}^2 - \mathbf{E}^2) = \frac{1}{2}(a^2 - b^2), \quad G = \frac{1}{4}F^{\mu\nu}F_{\mu\nu}^* = -\mathbf{E} \cdot \mathbf{B} = \sigma ab, \quad (2)$$

where σ denotes the sign of G . As will be shown later, the formulation in terms of a and b , instead of F and G or \mathbf{E} and \mathbf{B} , has the advantage to facilitate the expansion of the effective Lagrangian as a series of b .

The parameters a and b can be used to classify the cases of constant electromagnetic fields, as shown in Fig. 1. The sign of the Maxwell scalar F determines which field is stronger between the electric and magnetic fields, dividing the ab -plane into two regions: the upper left where the electric field is stronger and the lower right where the magnetic field is. The condition $G = 0$ shrinks each region to its attached coordinate axis. The cases with $G = 0$ are called wrenchless, while the fields with $G \neq 0$ are said to have an electromagnetic wrench [4]. In the wrenchless case, an appropriate Lorentz transformation can remove the weaker field between the magnetic field and the electric field [30]. Thus, the a -axis (b -axis) in Fig. 1 represents the condition of essentially being under a magnetic (electric) field; of course, it includes the case of a pure magnetic (electric) field. In studying the vacuum birefringence of astrophysical relevance, the magnetic field is much stronger than the electric field, and thus the region of $a \gg b$ in Fig. 1 is of our interests.

B. Integral expression of $\mathcal{L}^{(1)}(a, b)$ and closed expression of $\mathcal{L}^{(1)}(a, 0)$

The physics of the vacuum in intense electromagnetic fields has been studied with the effective Lagrangian, which is obtained by integrating out the matter field degrees of freedom in the complete Lagrangian [31]. In the effective Lagrangian, the term other than the free-field part, the Maxwell theory ($\mathcal{L}^{(0)}(a, b) = (b^2 - a^2)/2$), is responsible for the phenomena such as pair production, vacuum birefringence, photon splitting, etc. As the term is dominantly contributed from the one-loop [32–34] at least for the magnetic field strengths of astrophysical relevance, we consider the effective Lagrangian up to the one-loop:

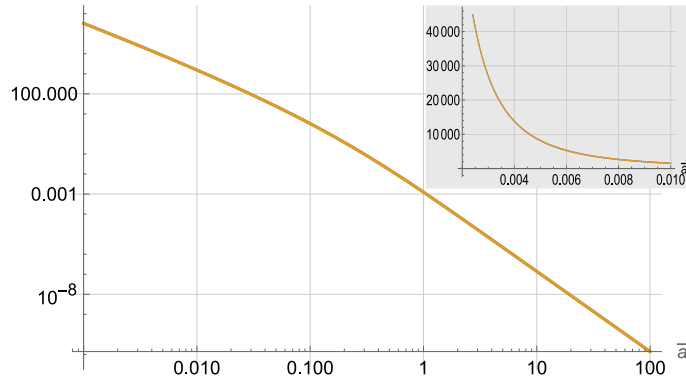


Figure 2. Comparison of the integral and closed expressions of $\bar{\mathcal{L}}^{(1)}(\bar{a}, 0)$. The integral expression is (5) with $\tilde{b} = 0$, and the closed one is (7). The plotted values are in units of $m^4/8\pi^2$. The parameter \bar{a} ranges from 0.001 to 100, corresponding to B/B_c from 500 to 0.005 for the purely magnetic case. The inset shows the values in linear scale for the range of \bar{a} from 0.002 to 0.01. The plots of the two expressions perfectly overlap each other.

$$\mathcal{L}_{\text{eff}}(a, b) = \mathcal{L}^{(0)}(a, b) + \mathcal{L}^{(1)}(a, b) = \frac{b^2 - a^2}{2} + \mathcal{L}^{(1)}(a, b). \quad (3)$$

The one-loop contribution $\mathcal{L}^{(1)}(a, b)$ for the spinor QED is given as a proper-time integral [1–3]:

$$\mathcal{L}^{(1)}(a, b) = -\frac{1}{8\pi^2} \int_0^\infty ds \frac{e^{-m^2 s}}{s^3} \left\{ (eas) \coth(eas)(ebs) \cot(ebs) - \left[1 + \frac{(eas)^2 - (ebs)^2}{3} \right] \right\}, \quad (4)$$

where m is the electron mass, and $1 + (es)^2(a^2 - b^2)/3$ is subtracted to remove the zero-point energy and renormalize the charge and fields for yielding a finite physical quantity [3]. This expression can be rewritten in a form convenient for the case of $a \gg b$, i.e., $\tilde{b} = b/a \ll 1$:

$$\mathcal{L}^{(1)}(a, b) = \bar{\mathcal{L}}^{(1)}(\bar{a}, \tilde{b}) = \frac{m^4}{8\pi^2} \frac{1}{4\bar{a}^2} \int_0^\infty dz \frac{e^{-2\bar{a}z}}{z^3} \left[1 + \frac{z^2(1 - \tilde{b}^2)}{3} - \tilde{b}z^2 \coth(z) \cot(z\tilde{b}) \right], \quad (5)$$

where the dimensionless variable and parameters are

$$z = eas, \quad \bar{a} = \frac{m^2}{2ea}, \quad \bar{b} = \frac{m^2}{2eb}, \quad \tilde{b} = \frac{b}{a} = \frac{\bar{a}}{\bar{b}}. \quad (6)$$

For a pure magnetic field, $\bar{a} = (B_c/B)/2$ and $\bar{b} = \infty$, where $B_c = m^2/e = 4.4 \times 10^{13}$ gauss/ $\sqrt{4\pi}$ is the critical magnetic field strength.

This integral can be numerically evaluated as described in App. A, but an explicit closed expression can be favored for theoretical analysis. For the case of $b = 0$, an explicit expression was obtained either by the dimensional regularization of (4) [25] or by the Schwinger-DeWitt in-out formalism combined with Γ -function regularization [27]:

$$\bar{\mathcal{L}}^{(1)}(\bar{a}, 0) \equiv \frac{m^4}{8\pi^2 \bar{a}^2} H(\bar{a}) = \frac{m^4}{8\pi^2 \bar{a}^2} \left[\zeta'(-1, \bar{a}) - \frac{1}{12} + \frac{\bar{a}^2}{4} - \left(\frac{1}{12} - \frac{\bar{a}}{2} + \frac{\bar{a}^2}{2} \right) \ln \bar{a} \right], \quad (7)$$

where $\zeta(s, \bar{a})$ is the Hurwitz zeta function, and $\zeta'(-1, \bar{a}) = d\zeta(s, \bar{a})/ds|_{s=-1}$ [35] (See App. B for more details.). This expression perfectly matches the numerical evaluation of (5) with $\tilde{b} = 0$, as shown in Fig. 2. We use this analytic expression of $\bar{\mathcal{L}}^{(1)}(\bar{a}, 0)$ to express $\bar{\mathcal{L}}^{(1)}(\bar{a}, \tilde{b})$ as a series of $\tilde{b} = b/a$, as shown in the next section.

C. Expansion of $\bar{\mathcal{L}}^{(1)}(\bar{a}, \tilde{b})$ in \tilde{b}

In the magnetosphere of pulsars, the magnetic field is much stronger than the electric field, and thus $a \gg b$, or equivalently $\bar{a} \ll \tilde{b}$, from (1) and (2). For example, a pulsar model [21] gives \tilde{b} ($= b/a$) as a function decreasing with the distance from the pulsar center: $\tilde{b}(R) \leq 0.2$ and $\tilde{b}(10R) \leq 0.02$, where R is the radius of the pulsar. For such a condition, the expansion of $\bar{\mathcal{L}}^{(1)}(\bar{a}, \tilde{b})$ in \tilde{b} is useful for analysis.

In the integral expression of $\bar{\mathcal{L}}^{(1)}(\bar{a}, \tilde{b})$ (5), $\cot(\tilde{b}z)$ has poles at $z = n\pi/\tilde{b}$ ($n = 1, 2, \dots$), which may apparently make the integral diverge. However, only the Cauchy principal value of the integral is relevant for vacuum birefringence, and the symmetric behavior of the cotangent function around the poles prevents the principal value from diverging. Furthermore, if $\exp(-2\bar{a}z)$ suppresses the integrand sufficiently much before the first pole, i.e., $1/(2\bar{a}) \ll \pi/\tilde{b}$, or equivalently $\tilde{b} \gg 1/(2\pi)$, an asymptotic expression valid for $\tilde{b} \gg 1/(2\pi)$ can be obtained. To proceed, we substitute the series form of $(\tilde{b}z) \cdot \cot(\tilde{b}z)$ in (5) (4.19.6 of [35]):

$$(\tilde{b}z) \cdot \cot(\tilde{b}z) = \sum_{n=0}^{\infty} \frac{B_{2n}(-1)^n (2\tilde{b}z)^{2n}}{(2n)!}, \quad (8)$$

where B_{2n} are the Bernoulli numbers. The series is convergent only for $|\tilde{b}z| < \pi$ due to the nearest poles at $\tilde{b}z = \pm\pi$. Upon substitution, the contribution outside the region of convergence asymptotically vanishes as $\tilde{b} \rightarrow \infty$. Then, the integral in (5) is written as

$$\int_0^{\infty} dz \frac{e^{-2\bar{a}z}}{z^3} \left\{ 1 + \frac{z^2(1-\tilde{b}^2)}{3} - z \coth(z) \sum_{n=0}^{\infty} \frac{(-1)^n B_{2n} (2\tilde{b}z)^{2n}}{(2n)!} \right\}. \quad (9)$$

To evaluate the integral, we use the integral representation of $H(\bar{a})$ in (7), which is derived by comparing (7) with (B1):

$$H(\bar{a}) = \frac{1}{4} \int_0^{\infty} dz \frac{e^{-2\bar{a}z}}{z^3} \left\{ 1 + \frac{z^2}{3} - z \coth(z) \right\}. \quad (10)$$

Differentiating (10) $2n$ times by \bar{a} yields a useful formula:

$$\left(\frac{d}{d\bar{a}} \right)^{2n} H(\bar{a}) \equiv H^{(2n)}(\bar{a}) = \frac{2^{2n}}{4} \int_0^{\infty} dz \frac{e^{-2\bar{a}z}}{z^3} \left\{ 1 + \frac{z^2}{3} - z \coth(z) \right\} z^{2n}, \quad (11)$$

of which closed form is given as (See App. C for the derivation)

$$H^{(2n)}(\bar{a}) = \psi^{(2n-2)}(\bar{a}) + \frac{1}{12} \frac{\Gamma(2n)}{\bar{a}^{2n}} + \frac{1}{2} \frac{\Gamma(2n-1)}{\bar{a}^{2n-1}} + \frac{\Gamma(2n-2)}{\bar{a}^{2n-2}} \theta(n-2) - \delta_{n1} \ln \bar{a}, \quad (n \geq 1), \quad (12)$$

where $\psi^{(m)}(\bar{a})$ is the polygamma function. By using (11) and (12) and the integral representation of the Γ function, one can integrate (9) term-by-term to obtain an asymptotic series of $\bar{\mathcal{L}}^{(1)}(\bar{a}, \tilde{b})$:

$$\begin{aligned} \bar{\mathcal{L}}^{(1)}(\bar{a}, \tilde{b}) &= \frac{m^4}{8\pi^2} \left[\frac{H(\bar{a})}{\bar{a}^2} + \left(\frac{1}{144\bar{a}^4} - \frac{H^{(2)}(\bar{a})}{12\bar{a}^2} \right) \tilde{b}^2 \right] \\ &+ \frac{m^4}{8\pi^2} \sum_{n=2}^{\infty} (-1)^n B_{2n} \left[\frac{H^{(2n)}(\bar{a})}{(2n)! \bar{a}^{2n}} - \frac{1}{2n(2n-1)(2n-2)\bar{a}^{2n}} - \frac{1}{24n\bar{a}^{2n+2}} \right] \tilde{b}^{2n}, \end{aligned} \quad (13)$$

in which all the terms are given in terms of special functions. Thus, (13) provides a systematic explicit expression of $\bar{\mathcal{L}}^{(1)}(\bar{a}, \tilde{b})$ in powers of $\tilde{b} = b/a$ for an arbitrary value of \bar{a} . For example, the first three leading orders are given as

$$\begin{aligned} \bar{\mathcal{L}}^{(1)}(\bar{a}, \tilde{b}) &= \frac{m^4}{8\pi^2} \frac{1}{\bar{a}^2} \left[\zeta'(-1, \bar{a}) - \frac{1}{12} + \frac{\bar{a}^2}{4} - \left(\frac{1}{12} - \frac{\bar{a}}{2} + \frac{\bar{a}^2}{2} \right) \ln \bar{a} \right] \\ &+ \frac{m^4}{8\pi^2} \left(-\frac{1}{24\bar{a}^3} + \frac{\ln \bar{a} - \psi^{(0)}(\bar{a})}{12\bar{a}^2} \right) \tilde{b}^2 + \frac{m^4}{8\pi^2} \left(-\frac{1}{720\bar{a}^5} - \frac{\psi^{(2)}(\bar{a})}{720\bar{a}^2} \right) \tilde{b}^4 + O(\tilde{b}^6). \end{aligned} \quad (14)$$

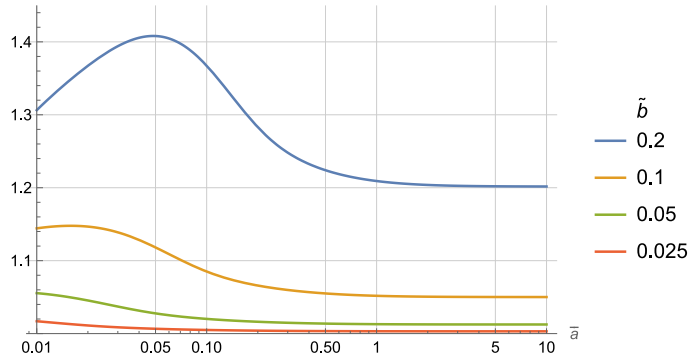


Figure 3. $\bar{\mathcal{L}}^{(1)}(\bar{a}, \tilde{b})/\bar{\mathcal{L}}^{(1)}(\bar{a}, 0)$ for $\tilde{b} = 0.2, 0.1, 0.05, 0.025$. $\bar{\mathcal{L}}^{(1)}(\bar{a}, \tilde{b})$ was obtained by the direct integration of (5), in which the first 10 poles were included.

A similar expansion in $K = -16a^2b^2$ was made by Heyl and Hernquist to yield the explicit expressions of the lowest few orders [36].

When both electric and magnetic fields are highly subcritical, i.e., $\bar{a} \gg 1$ and $\bar{b} \gg 1$ hold, the lowest order can be obtained from the expansion up to $O(\tilde{b}^4)$, and the second lowest from the expansion up to $O(\tilde{b}^6)$:

$$\begin{aligned} \bar{\mathcal{L}}^{(1)}(\bar{a}, \tilde{b}) &= \frac{m^4}{8\pi^2} \frac{1}{\bar{a}^4} \left[\frac{1}{720} + \frac{\tilde{b}^2}{144} + \frac{\tilde{b}^4}{720} \right] + \frac{m^4}{8\pi^2} \frac{1}{\bar{a}^6} \left[-\frac{1}{5040} - \frac{\tilde{b}^2}{1440} + \frac{\tilde{b}^4}{1440} + \frac{\tilde{b}^6}{5040} \right] \\ &= \frac{m^4}{8\pi^2} \left[\frac{1}{720\bar{a}^4} + \frac{1}{144\bar{a}^2\tilde{b}^2} + \frac{1}{720\tilde{b}^4} \right] + \frac{m^4}{8\pi^2} \left[-\frac{1}{5040\bar{a}^6} - \frac{1}{1440\bar{a}^4\tilde{b}^2} + \frac{1}{1440\bar{a}^2\tilde{b}^4} + \frac{1}{5040\tilde{b}^6} \right] \end{aligned} \quad (15)$$

The term with the first bracket is written in terms of \mathbf{E} and \mathbf{B} as

$$\frac{e^4}{360\pi^2 m^4} [(\mathbf{B}^2 - \mathbf{E}^2)^2 + 7(\mathbf{E} \cdot \mathbf{B})^2], \quad (16)$$

which was obtained by Heisenberg and Euler [1], and Schwinger [3].

It needs to be mentioned that the one-loop effective Lagrangian $\mathcal{L}^{(1)}(a, b)$ (4) can be expressed as a convergent series of which terms are some special functions of a and b [37–39]. The expansion may be exact but is not very convenient for the condition of an arbitrarily strong magnetic field combined with a weaker electric field because the expansion needs an infinite sum. The convergence of the sum is slow, and thus its evaluation needs acceleration techniques [38]. In this regards, the expansion (14) is more convenient for theoretical analysis.

D. Behavior of $\bar{\mathcal{L}}^{(1)}(\bar{a}, \tilde{b})$ and the validity of its expansion expression

The exact dependence of $\bar{\mathcal{L}}^{(1)}(\bar{a}, \tilde{b})$ with \tilde{b} can be investigated by numerically evaluating the integral expression (5), as described in App. A. As $\bar{\mathcal{L}}^{(1)}(\bar{a}, 0)$ is completely known, the ratio $\bar{\mathcal{L}}^{(1)}(\bar{a}, \tilde{b})/\bar{\mathcal{L}}^{(1)}(\bar{a}, 0)$ represents the dependence on \tilde{b} alone. In Fig. 3, the offset difference of $\bar{\mathcal{L}}^{(1)}(\bar{a}, \tilde{b})$ from $\bar{\mathcal{L}}^{(1)}(\bar{a}, 0)$ increases with \tilde{b} . Furthermore, additional significant differences appear as \bar{a} decreases below certain onset values. For example, when $\tilde{b} = 0.2$, the ratio is close 1.2 until \bar{a} decreases to 1, but, as \bar{a} decreases below 1, it significantly increases and then decreases. When \tilde{b} is smaller, the behavior is similar except that the offset difference is smaller, and the onset value of \bar{a} decreases. This additional difference is considered to be attributed to the pair production. When $1/(2\bar{a}) \gtrsim \pi/\tilde{b}$, or equivalently $\tilde{b} \lesssim 1/(2\pi)$, the contribution from the first pole of the cotangent function in (5) becomes significant. As $\tilde{b} = E_{\text{cr}}/(2E)$ in the parallel field configuration, the condition $\tilde{b} \lesssim 1/(2\pi)$ implies the emergence of the pair production by the strong electric field. In such a case, the effective Lagrangian develops an imaginary part, which is accompanied by a variation in the real part, i.e., the additional difference in Fig. 3. It is similar to the anomalous dispersion near a resonance region in the linear optical response [40]. As the imaginary part gives the pair production probability, the plasma effects appears when the probability is sufficiently high. Then, it is no more pure vacuum birefringence. In our analysis, we focus on real part of the Lagrangian to study the pure vacuum birefringence.

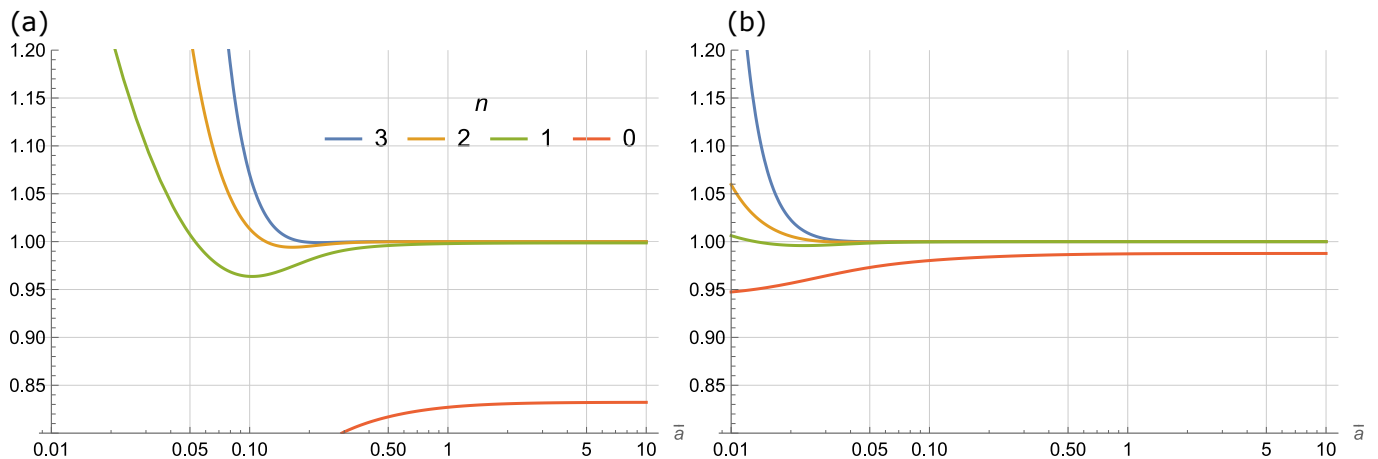


Figure 4. $\bar{\mathcal{L}}_{\text{exp}}^{(1)}(\bar{a}, \tilde{b}, n) / \bar{\mathcal{L}}_{\text{int}}^{(1)}(\bar{a}, \tilde{b})$ for $n = 0, 1, 2, 3$ when (a) $\tilde{b} = 0.2$ and (b) $\tilde{b} = 0.05$. $\bar{\mathcal{L}}_{\text{exp}}^{(1)}(\bar{a}, \tilde{b}, n)$ is the expansion (13) up to $O(\tilde{b}^{2n})$, and $\bar{\mathcal{L}}_{\text{int}}^{(1)}(\bar{a}, \tilde{b})$ is the numerical evaluation of (5), including the first 10 poles.

By using the numerical evaluation of $\bar{\mathcal{L}}^{(1)}(\bar{a}, \tilde{b})$, we can find the parameter range in which the expansion (13) is accurate. The ratio $\bar{\mathcal{L}}_{\text{exp}}^{(1)}(\bar{a}, \tilde{b}, n) / \bar{\mathcal{L}}_{\text{int}}^{(1)}(\bar{a}, \tilde{b})$ is plotted for $n = 0, 1, 2, 3$ and $\tilde{b} = 0.2, 0.05$, where $\bar{\mathcal{L}}_{\text{exp}}^{(1)}(\bar{a}, \tilde{b}, n)$ is the expansion (13) up to $O(\tilde{b}^{2n})$, and $\bar{\mathcal{L}}_{\text{int}}^{(1)}(\bar{a}, \tilde{b})$ is the numerical evaluation of (5). In Fig. 4(a), $\bar{\mathcal{L}}_{\text{exp}}^{(1)}(\bar{a}, \tilde{b} = 0.2, n \geq 1)$ is accurate within 1% for $\bar{a} \geq 0.3$. The 1%-accuracy threshold of \bar{a} , denoted by $\bar{a}_{1\%}$, decreases slightly as n increases, but a higher- n expansion blows up faster below $\bar{a}_{1\%}$; a typical behavior of the Taylor expansion. The $n = 0$ expansion, corresponding to the effective Lagrangian with $\tilde{b} = 0$, has an error larger than 17%. At a lower value of $\tilde{b} = 0.05$, the overall behavior is similar to the case of $\tilde{b} = 0.2$, but $\bar{a}_{1\%}$ is lowered to 0.025, and the minimum error of the $n = 0$ expansion decreases to 2%, as shown in Fig. 4(b). In practice, the $n = 2$ expansion can be a reasonable choice for analysis, showing $\bar{a}_{1\%} = 0.1$ for $\tilde{b} = 0.2$ ($B \leq 5B_{\text{cr}}$ and $E \leq E_{\text{cr}}$) and $\bar{a}_{1\%} = 0.02$ for $\tilde{b} = 0.05$ ($B \leq 25B_{\text{cr}}$ and $E \leq 1.25E_{\text{cr}}$). Noting that the expansion is not accurate when the pair production is significant, one may roughly estimate a threshold value of \bar{a} like $\bar{a}_{1\%}$ by requiring $\tilde{b}/(2\bar{a}_{\text{thres}}) \simeq 1$. As $\tilde{b}/(2\bar{a}) = E/E_{\text{cr}}$ in the parallel field configuration, the expansion would not be accurate when this ratio is the order of unity. In Fig. 4, the threshold values $\bar{a}_{1\%}$ are close to the estimation $\bar{a}_{\text{thres}} = \tilde{b}/2$.

III. RESPONSE OF THE VACUUM IN STRONG ELECTROMAGNETIC FIELDS

In contrast to the classical vacuum, the quantum vacuum in electromagnetic fields behaves as a medium, of which response is quantified by the polarization (\mathbf{P}) and the magnetization (\mathbf{M}), or equivalently by the electric induction (\mathbf{D}) and magnetic field strength (\mathbf{H}). These quantities can be obtained by considering the variation of the effective Lagrangian with respect to that of the electromagnetic field [1, 41]:

$$\mathbf{D} = \mathbf{E} + \mathbf{P} = \frac{\partial \mathcal{L}_{\text{eff}}}{\partial \mathbf{E}} = \mathbf{E} + \frac{\partial \mathcal{L}^{(1)}}{\partial \mathbf{E}}, \quad \mathbf{H} = \mathbf{B} - \mathbf{M} = -\frac{\partial \mathcal{L}_{\text{eff}}}{\partial \mathbf{B}} = \mathbf{B} - \frac{\partial \mathcal{L}^{(1)}}{\partial \mathbf{B}}. \quad (17)$$

In this section, we derive expressions of \mathbf{P} and \mathbf{M} for an arbitrary $\mathcal{L}^{(1)}(a, b)$ and use the result to obtain the permittivity and permeability tensors for weak low-frequency ($\omega \ll m$) probe fields. These tensors are necessary to analyze the vacuum birefringence in the next section. These results can be obtained also in an explicitly Lorentz covariant manner by using photon polarization tensors [4, 29, 42, 43].

A. Polarization and magnetization of the vacuum in uniform electric and magnetic fields

The effective Lagrangian is a function of a and b (1) and (2), and thus we consider the variation of a general differentiable function $f(a, b)$:

$$\delta f = \delta a \cdot \partial_a f + \delta b \cdot \partial_b f. \quad (18)$$

As a and b are functions of F and G , the variations δa and δb can be written in terms of the variations δF and δG :

$$\delta a = \frac{\partial a}{\partial F} \delta F + \frac{\partial a}{\partial G} \delta G, \quad \delta b = \frac{\partial b}{\partial F} \delta F + \frac{\partial b}{\partial G} \delta G. \quad (19)$$

In turn, the variations of δF and δG can also be written in terms of $\delta \mathbf{E}$ and $\delta \mathbf{B}$:

$$\delta F = \frac{\partial F}{\partial \mathbf{E}} \cdot \delta \mathbf{E} + \frac{\partial F}{\partial \mathbf{B}} \cdot \delta \mathbf{B}, \quad \delta G = \frac{\partial G}{\partial \mathbf{E}} \cdot \delta \mathbf{E} + \frac{\partial G}{\partial \mathbf{B}} \cdot \delta \mathbf{B}. \quad (20)$$

Thus, using the chain rules, the coefficients in these variations can be calculated by using (1) and (2) to express δf in terms of $\delta \mathbf{E}$ and $\delta \mathbf{B}$:

$$\delta f = \delta \mathbf{E} \cdot \left(-\mathbf{E} \hat{S} - \mathbf{B} \hat{A} \right) f + \delta \mathbf{B} \cdot \left(\mathbf{B} \hat{S} - \mathbf{E} \hat{A} \right) f, \quad (21)$$

where

$$\hat{S} = \frac{(a \cdot \partial_a - b \cdot \partial_b)}{a^2 + b^2} = \partial_F, \quad \hat{A} = \frac{\sigma(b \cdot \partial_a + a \cdot \partial_b)}{a^2 + b^2} = \partial_G, \quad \hat{S} \hat{A} = \hat{A} \hat{S} = \partial_F \partial_G. \quad (22)$$

The operators \hat{S} and \hat{A} are symmetric and antisymmetric under the parity inversion, respectively. Note that $(a^2 + b^2) \hat{S}$ measures the difference of homogeneity of polynomials such that $(a^2 + b^2) \hat{S}(a^m b^n) = (m - n)(a^m b^n)$, while $(a^2 + b^2) \hat{A}$ measures the mixed homogeneity of polynomials such that $(a^2 + b^2) \hat{A}(a^m b^n) = (mb^2 + na^2)(a^{m-1} b^{n-1})$. In addition, $(a^2 + b^2) \hat{S}$ preserves the polynomial order (m, n) , while $(a^2 + b^2) \hat{A}$ changes it to $(m - 1, n + 1)$ and $(m + 1, n - 1)$ while maintaining the sum of the orders of a and b . Replacing f with $\mathcal{L}^{(1)}$ and using (17), one can obtain \mathbf{P} and \mathbf{M} from $\mathcal{L}^{(1)}(a, b)$:

$$\mathbf{P} = \frac{\partial \mathcal{L}^{(1)}}{\partial \mathbf{E}} = -\mathbf{E} \hat{S} \mathcal{L}^{(1)} - \mathbf{B} \hat{A} \mathcal{L}^{(1)}, \quad \mathbf{M} = \frac{\partial \mathcal{L}^{(1)}}{\partial \mathbf{B}} = \mathbf{B} \hat{S} \mathcal{L}^{(1)} - \mathbf{E} \hat{A} \mathcal{L}^{(1)}. \quad (23)$$

Despite the appearance, this relation is not linear in \mathbf{E} and \mathbf{B} , as $\hat{S} \mathcal{L}^{(1)}$ and $\hat{A} \mathcal{L}^{(1)}$ are nonlinear functions of \mathbf{E} and \mathbf{B} .

B. Permittivity and permeability tensors for weak low-frequency probe fields

The material-like vacuum with the nonlinear response relation (23) affects the propagation of photons. When the photon energy is much smaller than the electron's rest mass energy ($\omega \ll m = 0.5 \text{ MeV}$), the photon can be treated as a weak perturbation field (probe field) added to the strong background field [44, 45]. Then, \mathbf{E} , \mathbf{B} , \mathbf{D} , \mathbf{H} , \mathbf{P} , and \mathbf{M} can be decomposed as

$$\mathbf{A} = \mathbf{A}_0 + \delta \mathbf{A}, \quad (24)$$

where \mathbf{A}_0 ($\delta \mathbf{A}$) refers to the quantities of the background (probe) field. Furthermore, as \mathbf{A}_0 is uniform, while $\delta \mathbf{A}$ is varying, the relation (17) should be satisfied separately between the uniform and varying quantities:

$$\mathbf{D}_0 = \mathbf{E}_0 + \mathbf{P}_0, \quad \mathbf{H}_0 = \mathbf{B}_0 - \mathbf{M}_0, \quad (25)$$

$$\delta \mathbf{D} = \delta \mathbf{E} + \delta \mathbf{P}, \quad \delta \mathbf{H} = \delta \mathbf{B} - \delta \mathbf{M}. \quad (26)$$

Then, $\delta \mathbf{D}$ and $\delta \mathbf{H}$ can be obtained by varying the relation (23) around $(\mathbf{E}_0, \mathbf{B}_0)$, for which the formula (21) is convenient. A straightforward but lengthy calculation yields the linear relations among the varying quantities relevant to the probe field:

$$\delta \mathbf{D} = \boldsymbol{\epsilon}_E \cdot \delta \mathbf{E} + \boldsymbol{\epsilon}_B \cdot \delta \mathbf{B}, \quad \delta \mathbf{H} = \bar{\boldsymbol{\mu}}_B \cdot \delta \mathbf{B} + \bar{\boldsymbol{\mu}}_E \cdot \delta \mathbf{E}, \quad (27)$$

where $\boldsymbol{\epsilon}_E$, $\boldsymbol{\epsilon}_B$, $\bar{\boldsymbol{\mu}}_B$, and $\bar{\boldsymbol{\mu}}_E$ are 3-by-3 tensors. Their components are as follows:

$$\epsilon_{E,ij} = \delta_{ij}(1 - \mathcal{L}_S^{(1)}) + \left[E_{0i}E_{0j}\mathcal{L}_{SS}^{(1)} + (E_{0i}B_{0j} + B_{0i}E_{0j})\mathcal{L}_{SA}^{(1)} + B_{0i}B_{0j}\mathcal{L}_{AA}^{(1)} \right], \quad (28)$$

$$\epsilon_{B,ij} = -\delta_{ij}\mathcal{L}_S^{(1)} + \left[-E_{0i}B_{0j}\mathcal{L}_{SS}^{(1)} + (E_{0i}E_{0j} - B_{0i}B_{0j})\mathcal{L}_{SA}^{(1)} + B_{0i}E_{0j}\mathcal{L}_{AA}^{(1)} \right], \quad (29)$$

$$\bar{\mu}_{B,ij} = \delta_{ij}(1 - \mathcal{L}_S^{(1)}) + \left[-B_{0i}B_{0j}\mathcal{L}_{SS}^{(1)} + (B_{0i}E_{0j} + E_{0i}B_{0j})\mathcal{L}_{SA}^{(1)} - E_{0i}E_{0j}\mathcal{L}_{AA}^{(1)} \right], \quad (30)$$

$$\bar{\mu}_{E,ij} = \delta_{ij}\mathcal{L}_A^{(1)} + \left[B_{0i}E_{0j}\mathcal{L}_{SS}^{(1)} + (B_{0i}B_{0j} - E_{0i}E_{0j})\mathcal{L}_{SA}^{(1)} - E_{0i}B_{0j}\mathcal{L}_{AA}^{(1)} \right], \quad (31)$$

where

$$\mathcal{L}_S^{(1)} = \hat{S}_0\mathcal{L}^{(1)}, \quad \mathcal{L}_A^{(1)} = \hat{A}_0\mathcal{L}^{(1)}, \quad \mathcal{L}_{SS}^{(1)} = \left(\hat{S}\hat{S} \right)_0 \mathcal{L}^{(1)}, \quad \mathcal{L}_{SA}^{(1)} = \left(\hat{S}\hat{A} \right)_0 \mathcal{L}^{(1)}, \quad \mathcal{L}_{AA}^{(1)} = \left(\hat{A}\hat{A} \right)_0 \mathcal{L}^{(1)}. \quad (32)$$

Here, the subscript 0 means that \hat{S} and \hat{A} are evaluated at $(\mathbf{E}_0, \mathbf{B}_0)$. Note that these formulas are valid for any effective Lagrangian. From now on, we shall focus on the Heisenberg-Euler and Schwinger effective Lagrangian (4).

The tensors $\boldsymbol{\epsilon}_B$ and $\bar{\boldsymbol{\mu}}_E$ represent the magneto-electric response to the probe field, in which a magnetic (electric) field induces polarization (magnetization) [46], unlike usual dielectric and magnetic materials (See [47, 48] for the recent studies of the magneto-electric response in condensed matter). Such response disappears as the background electric field vanishes: when $\mathbf{E}_0 = 0$, $\mathcal{L}_A^{(1)}$ and $\mathcal{L}_{SA}^{(1)}$ in (29,31) vanishes for the Lagrangian (4) to yield $\boldsymbol{\epsilon}_B = \bar{\boldsymbol{\mu}}_E = 0$.

The quantities in (32) have the complete information for the analysis of vacuum birefringence because they immediately lead to the permittivity and permeability for an arbitrary background field configuration through (28,29,30,31). By using the expansion (14), we can obtain the formulas of (32) contributed from each order of \bar{b} . For example, the contributions from the lowest three orders are shown in Tabs. I, II, and III. In Tab. I, the dependence on \bar{b} appears due to the $b \cdot \partial_a$ term in \hat{A} although $\bar{\mathcal{L}}^{(1)}(\bar{a}, 0)$ does not depend on \bar{b} . As the combined field of the background field and the probe field is not wrenchless in general, the expression of $\bar{\mathcal{L}}^{(1)}(\bar{a}, \bar{b} \neq 0)$ is necessary for wrenchless background fields.

For the case of $b = 0$ with an arbitrary value of a , i.e., the wrenchless case, the exact expressions of $\mathcal{L}_S^{(1)}$, $\mathcal{L}_A^{(1)}$, $\mathcal{L}_{SS}^{(1)}$, $\mathcal{L}_{SA}^{(1)}$, and $\mathcal{L}_{AA}^{(1)}$ can be obtained first by combining the results in Tabs. I and II and then by taking the limit of $\bar{b} = \infty$. Higher order contributions are absent in this case. The results are shown in Tab. IV. The same results were obtained by Karbstein et al. [43], who expanded the one-loop effective action up to the second order of the probe field and specified the calculation to the wrenchless case.

The weak-field limit of the quantities in (32) can be obtained by combining the results in Tabs. I, II, and III, and finding the asymptotic form for the limit of $\bar{a}, \bar{b} \rightarrow \infty$. Alternatively, the weak-field limit of the effective Lagrangian (15) can be used to evaluate $\mathcal{L}_S^{(1)}$, $\mathcal{L}_A^{(1)}$, $\mathcal{L}_{SS}^{(1)}$, $\mathcal{L}_{SA}^{(1)}$, and $\mathcal{L}_{AA}^{(1)}$:

$$\mathcal{L}_S^{(1)} = \frac{e^2}{360\pi^2} \left(\frac{1}{\bar{a}^2} - \frac{1}{\bar{b}^2} \right), \quad \mathcal{L}_A^{(1)} = \frac{7e^2\sigma}{720\bar{a}\bar{b}\pi^2}, \quad (33)$$

$$\mathcal{L}_{SS}^{(1)} = \frac{e^4}{45m^4\pi^2}, \quad \mathcal{L}_{SA}^{(1)} = 0, \quad \mathcal{L}_{AA}^{(1)} = \frac{7e^4}{180m^4\pi^2}, \quad (34)$$

which are obtained with the quantities of the first bracket in (15) only. When $\bar{b} = \infty$, these expressions yields the permittivity and permeability tensors obtained by Adler for the case of a weak magnetic field [45]. If the quantities of the second bracket in (15) is used, higher-order contributions are obtained.

$\mathcal{L}_S^{(1)}$	$-\frac{\bar{b}^2 e^2}{24(\bar{a}^2 + \bar{b}^2)\pi^2}$	$6\bar{a}^2 - 6\ln(2\pi)\bar{a} + 12\ln(\Gamma(\bar{a}))\bar{a} + (2 - 6\bar{a})\ln(\bar{a}) - 24\zeta'(-1, \bar{a}) + 1$
$\mathcal{L}_A^{(1)}$	$-\frac{\bar{a}\bar{b}e^2\sigma}{24(\bar{a}^2 + \bar{b}^2)\pi^2}$	$6\bar{a}^2 - 6\ln(2\pi)\bar{a} + 12\ln(\Gamma(\bar{a}))\bar{a} + (2 - 6\bar{a})\ln(\bar{a}) - 24\zeta'(-1, \bar{a}) + 1$
$\mathcal{L}_{SS}^{(1)}$	$\frac{\bar{a}^2\bar{b}^4 e^4}{3(\bar{a}^2 + \bar{b}^2)^3 m^4 \pi^2}$	$6(\psi^{(0)}(\bar{a}) + 1)\bar{a}^4 + 6\bar{a}^4 + 9\ln(\bar{a})\bar{a}^3 - 12\bar{a}^3 - 6\bar{b}^2\bar{a}^2 - 4\ln(\bar{a})\bar{a}^2 + 6\bar{b}^2(\psi^{(0)}(\bar{a}) + 1)\bar{a}^2 + 48\zeta'(-1, \bar{a})\bar{a}^2 - \bar{a}^2 - 3\bar{b}^2\ln(\bar{a})\bar{a} - 3(5\bar{a}^2 + \bar{b}^2)(2\bar{a} - \ln(2\pi) + 2\ln(\Gamma(\bar{a})) - 1)\bar{a} + \bar{b}^2$
$\mathcal{L}_{SA}^{(1)}$	$\frac{\bar{a}^3\bar{b}^3 e^4 \sigma}{3(\bar{a}^2 + \bar{b}^2)^3 m^4 \pi^2}$	$-12\bar{a}^4 + 3\ln(\bar{a})\bar{a}^3 + 9\ln(2\pi)\bar{a}^3 - 18\ln(\Gamma(\bar{a}))\bar{a}^3 + 3\bar{a}^3 - 2\ln(\bar{a})\bar{a}^2 + 6(\bar{a}^2 + \bar{b}^2)\psi^{(0)}(\bar{a})\bar{a}^2 + 3\bar{b}^2\bar{a} - 9\bar{b}^2\ln(\bar{a})\bar{a} - 3\bar{b}^2\ln(2\pi)\bar{a} + 6\bar{b}^2\ln(\Gamma(\bar{a}))\bar{a} + 2\bar{b}^2 + 2\bar{b}^2\ln(\bar{a}) + 24(\bar{a}^2 - \bar{b}^2)\zeta'(-1, \bar{a})$
$\mathcal{L}_{AA}^{(1)}$	$\frac{\bar{a}^2\bar{b}^2 e^4 \sigma^2}{6(\bar{a}^2 + \bar{b}^2)^3 m^4 \pi^2}$	$-18\bar{a}^6 + 12\ln(2\pi)\bar{a}^5 - 24\ln(\Gamma(\bar{a}))\bar{a}^5 + 6\bar{a}^5 - 2\ln(\bar{a})\bar{a}^4 + 12(\bar{a}^2 + \bar{b}^2)\psi^{(0)}(\bar{a})\bar{a}^4 + \bar{a}^4 + 6\bar{b}^2\bar{a}^3 - 18\bar{b}^2\ln(\bar{a})\bar{a}^3 - 6\bar{b}^2\ln(2\pi)\bar{a}^3 + 12\bar{b}^2\ln(\Gamma(\bar{a}))\bar{a}^3 - 6\bar{b}^4\bar{a}^2 + 4\bar{b}^2\bar{a}^2 + 4\bar{b}^2\ln(\bar{a})\bar{a}^2 + 6\bar{b}^4\ln(\bar{a})\bar{a} + 6\bar{b}^4\ln(2\pi)\bar{a} - 12\bar{b}^4\ln(\Gamma(\bar{a}))\bar{a} - \bar{b}^4 - 2\bar{b}^4\ln(\bar{a}) + 24(\bar{a}^2 - \bar{b}^2)^2\zeta'(-1, \bar{a})$

Table I. Contribution to $\mathcal{L}_S^{(1)}$, $\mathcal{L}_A^{(1)}$, $\mathcal{L}_{SS}^{(1)}$, $\mathcal{L}_{SA}^{(1)}$, and $\mathcal{L}_{AA}^{(1)}$ from the $O(\bar{b}^0)$ term in the expansion of $\bar{\mathcal{L}}^{(1)}(\bar{a}, \bar{b})$ (14). Each factor in the second column should be multiplied to the corresponding formula in the third column. $\bar{b} = \bar{a}/\bar{b}$.

$\mathcal{L}_S^{(1)}$	$\frac{\bar{a}e^2}{48(\bar{a}^2 + \bar{b}^2)\pi^2}$	$2\psi^{(1)}(\bar{a})\bar{a}^2 - 4\ln(\bar{a})\bar{a} + 4\psi^{(0)}(\bar{a})\bar{a} - 2\bar{a} + 1$
$\mathcal{L}_A^{(1)}$	$\frac{e^2\sigma}{48\bar{b}(\bar{a}^2 + \bar{b}^2)\pi^2}$	$2\psi^{(1)}(\bar{a})\bar{a}^4 - 2\bar{a}^3 - \bar{a}^2 + 4\bar{b}^2\ln(\bar{a})\bar{a} - 4\bar{b}^2\psi^{(0)}(\bar{a})\bar{a} - 2\bar{b}^2$
$\mathcal{L}_{SS}^{(1)}$	$-\frac{\bar{a}^3\bar{b}^2 e^4}{12(\bar{a}^2 + \bar{b}^2)^3 m^4 \pi^2}$	$2\psi^{(2)}(\bar{a})\bar{a}^5 + 2\bar{b}^2\psi^{(2)}(\bar{a})\bar{a}^3 - 4\bar{a}^3 - \bar{a}^2 - 12\bar{b}^2\bar{a} - 16\bar{b}^2\ln(\bar{a})\bar{a} + 16\bar{b}^2\psi^{(0)}(\bar{a})\bar{a} + 3\bar{b}^2 + 2(3\bar{a}^4 + 7\bar{b}^2\bar{a}^2)\psi^{(1)}(\bar{a})$
$\mathcal{L}_{SA}^{(1)}$	$-\frac{\bar{a}^2\bar{b}e^4\sigma}{12(\bar{a}^2 + \bar{b}^2)^3 m^4 \pi^2}$	$2\psi^{(2)}(\bar{a})\bar{a}^7 + 2\bar{b}^2\psi^{(2)}(\bar{a})\bar{a}^5 - 4\bar{a}^5 - \bar{a}^4 - 8\bar{b}^2\bar{a}^3 - 8\bar{b}^2\ln(\bar{a})\bar{a}^3 + \bar{b}^2\bar{a}^2 + 4\bar{b}^4\bar{a} + 8\bar{b}^4\ln(\bar{a})\bar{a} + 8\bar{b}^2(\bar{a}^2 - \bar{b}^2)\psi^{(0)}(\bar{a})\bar{a} - 2\bar{b}^4 + 2(3\bar{a}^6 + 5\bar{b}^2\bar{a}^4 - 2\bar{b}^4\bar{a}^2)\psi^{(1)}(\bar{a})$
$\mathcal{L}_{AA}^{(1)}$	$-\frac{\bar{a}e^4\sigma^2}{12(\bar{a}^2 + \bar{b}^2)^3 m^4 \pi^2}$	$2\psi^{(2)}(\bar{a})\bar{a}^9 + 2\bar{b}^2\psi^{(2)}(\bar{a})\bar{a}^7 - 2\bar{a}^7 - 4\bar{b}^2\ln(\bar{a})\bar{a}^5 + 3\bar{b}^2\bar{a}^4 + 10\bar{b}^4\bar{a}^3 + 8\bar{b}^4\ln(\bar{a})\bar{a}^3 + \bar{b}^4\bar{a}^2 - 4\bar{b}^6\ln(\bar{a})\bar{a} + 4\bar{b}^2(\bar{a}^2 - \bar{b}^2)^2\psi^{(0)}(\bar{a})\bar{a} + 2\bar{b}^6 + 2(2\bar{a}^8 + \bar{b}^2\bar{a}^6 - 5\bar{b}^4\bar{a}^4)\psi^{(1)}(\bar{a})$

Table II. Contribution to $\mathcal{L}_S^{(1)}$, $\mathcal{L}_A^{(1)}$, $\mathcal{L}_{SS}^{(1)}$, $\mathcal{L}_{SA}^{(1)}$, and $\mathcal{L}_{AA}^{(1)}$ from the $O(\bar{b}^2)$ term in the expansion of $\bar{\mathcal{L}}^{(1)}(\bar{a}, \bar{b})$ (14). Each factor in the second column should be multiplied to the corresponding formula in the third column. $\bar{b} = \bar{a}/\bar{b}$.

IV. VACUUM BIREFRINGENCE FOR $\mathbf{B}_0 \parallel \mathbf{E}_0$ AND $|\mathbf{B}_0| \gg |\mathbf{E}_0|$

In this section, we work out the refractive indices and the polarization vectors for the case of a weak electric field added parallel to an arbitrarily strong magnetic field, as shown in Fig. 5. In such a configuration, $a = B_0$, $b = E_0$, and $\bar{a} = B_c/(2B_0)$. This configuration, looking too restrictive at a first glance, is actually general enough to include the non-parallel cases, too. By choosing an appropriate Lorentz transformation, one can transform non-perpendicular configurations into parallel ones and the perpendicular configuration into that of a pure magnetic one as far as the electric field is weaker than the magnetic field [4, 30]. However, the Lorentz transformation of the permittivity and permeability of anisotropic media is a highly non-trivial issue [49]. Furthermore, for the localized fields of the pulsar magnetosphere, such a parallelization of fields by a Lorentz transformation can be done only locally. We leave the resolution of these issues as future works.

The refractive indices and the associated polarization vectors are found by solving the Maxwell equations for the probe field. When the probe field is a plane wave with the propagation vector \mathbf{k} and the angular frequency ω ($\mathbf{k} = \omega\mathbf{n} = \omega n\hat{\mathbf{k}}$), the Maxwell equations for the probe field reduce to

$\mathcal{L}_S^{(1)}$	$\frac{\bar{a}e^2}{1440\bar{b}^2(\bar{a}^2 + \bar{b}^2)\pi^2}$	$\psi^{(3)}(\bar{a})\bar{a}^4 + 6\psi^{(2)}(\bar{a})\bar{a}^3 + 3$
$\mathcal{L}_A^{(1)}$	$\frac{e^2\sigma}{1440\bar{b}^3(\bar{a}^2 + \bar{b}^2)\pi^2}$	$\psi^{(3)}(\bar{a})\bar{a}^6 - \bar{a}^2 - 4\bar{b}^2 + 2(\bar{a}^5 - 2\bar{a}^3\bar{b}^2)\psi^{(2)}(\bar{a})$
$\mathcal{L}_{SS}^{(1)}$	$-\frac{\bar{a}^3 e^4}{360(\bar{a}^2 + \bar{b}^2)^3 m^4 \pi^2}$	$\psi^{(4)}(\bar{a})\bar{a}^7 + \bar{b}^2\psi^{(4)}(\bar{a})\bar{a}^5 + 3\bar{a}^2 + 15\bar{b}^2 + 24(\bar{a}^5 + 2\bar{b}^2\bar{a}^3)\psi^{(2)}(\bar{a}) + (11\bar{a}^6 + 15\bar{b}^2\bar{a}^4)\psi^{(3)}(\bar{a})$
$\mathcal{L}_{SA}^{(1)}$	$-\frac{\bar{a}^2 e^4 \sigma}{360\bar{b}(\bar{a}^2 + \bar{b}^2)^3 m^4 \pi^2}$	$\psi^{(4)}(\bar{a})\bar{a}^9 + \bar{b}^2\psi^{(4)}(\bar{a})\bar{a}^7 - 3\bar{a}^4 - 3\bar{b}^2\bar{a}^2 - 12\bar{b}^4 + 12(\bar{a}^7 + \bar{b}^2\bar{a}^5 - 2\bar{b}^4\bar{a}^3)\psi^{(2)}(\bar{a}) + (9\bar{a}^8 + 9\bar{b}^2\bar{a}^6 - 4\bar{b}^4\bar{a}^4)\psi^{(3)}(\bar{a})$
$\mathcal{L}_{AA}^{(1)}$	$-\frac{\bar{a}e^4\sigma^2}{360\bar{b}^2(\bar{a}^2 + \bar{b}^2)^3 m^4 \pi^2}$	$\psi^{(4)}(\bar{a})\bar{a}^{11} + \bar{b}^2\psi^{(4)}(\bar{a})\bar{a}^9 + (6\bar{a}^4 + \bar{b}^2\bar{a}^2 - 9\bar{b}^4)\psi^{(3)}(\bar{a})\bar{a}^6 + 9\bar{b}^2\bar{a}^4 + 9\bar{b}^4\bar{a}^2 + 12\bar{b}^6 + 6(\bar{a}^9 - 3\bar{b}^4\bar{a}^5 + 2\bar{b}^6\bar{a}^3)\psi^{(2)}(\bar{a})$

Table III. Contribution to $\mathcal{L}_S^{(1)}$, $\mathcal{L}_A^{(1)}$, $\mathcal{L}_{SS}^{(1)}$, $\mathcal{L}_{SA}^{(1)}$, and $\mathcal{L}_{AA}^{(1)}$ from the $O(\bar{b}^4)$ term in the expansion of $\bar{\mathcal{L}}^{(1)}(\bar{a}, \bar{b})$ (14). Each factor in the second column should be multiplied to the corresponding formula in the third column. $\bar{b} = \bar{a}/\bar{b}$.

$\mathcal{L}_S^{(1)}$	$-\frac{e^2}{24\pi^2}$	$6\bar{a}^2 - 6\ln(2\pi)\bar{a} + 12\ln(\Gamma(\bar{a}))\bar{a} + (2 - 6\bar{a})\ln(\bar{a}) - 24\zeta'(-1, \bar{a}) + 1$
$\mathcal{L}_{SS}^{(1)}$	$\frac{\bar{a}^2 e^4}{3m^4 \pi^2}$	$6\psi^{(0)}(\bar{a})\bar{a}^2 - 6\bar{a}^2 - 3\ln(\bar{a})\bar{a} + 3\ln(2\pi)\bar{a} - 6\ln(\Gamma(\bar{a}))\bar{a} + 3\bar{a} + 1$
$\mathcal{L}_{AA}^{(1)}$	$-\frac{\bar{a}e^4\sigma^2}{6m^4\pi^2}$	$6\bar{a}^3 - 6\ln(\bar{a})\bar{a}^2 - 6\ln(2\pi)\bar{a}^2 + 12\ln(\Gamma(\bar{a}))\bar{a}^2 + 2\psi^{(0)}(\bar{a})\bar{a} - 24\zeta^{(1,0)}(-1, \bar{a})\bar{a} + \bar{a} + 1$

Table IV. $\mathcal{L}_S^{(1)}$, $\mathcal{L}_{SS}^{(1)}$, and $\mathcal{L}_{AA}^{(1)}$ for $\tilde{b} = 0$. $\mathcal{L}_A^{(1)}$ and $\mathcal{L}_{SA}^{(1)}$ are null. Each factor in the second column should be multiplied to the corresponding formula in the third column. $\tilde{b} = \bar{a}/\tilde{b}$.

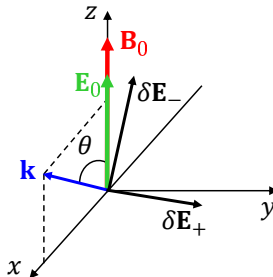


Figure 5. Configuration of the background fields (\mathbf{E}_0 , \mathbf{B}_0) and the probe field. The probe field has its propagation vector \mathbf{k} on the xz -plane and its two polarization vectors $\delta\mathbf{E}_\pm$ associated with the refractive indices n_\pm . Unless $E_0 = 0$ (thus $\epsilon_2 = 0$), $\delta\mathbf{E}_+$ is not along the y -axis, and $\delta\mathbf{E}_-$ is not on the xz -plane.

$$\omega\delta\mathbf{B} = \mathbf{k} \times \delta\mathbf{E}, \quad \omega\delta\mathbf{D} = -\mathbf{k} \times \delta\mathbf{H}. \quad (35)$$

By substituting (27) into these equations, we obtain a matrix-vector equation:

$$\epsilon_E \cdot \delta\mathbf{E} + \epsilon_B \cdot \mathbf{n} \times \delta\mathbf{E} + \mathbf{n} \times (\bar{\mu}_B \cdot \mathbf{n} \times \delta\mathbf{E} + \bar{\mu}_E \cdot \delta\mathbf{E}) = \mathbf{\Lambda} \cdot \delta\mathbf{E} = 0, \quad (36)$$

where $\mathbf{\Lambda}$ is a 3×3 matrix incorporating ϵ_E , ϵ_B , $\bar{\mu}_B$, $\bar{\mu}_E$, and \mathbf{n} . For this equation to have non-trivial solutions, $\det\mathbf{\Lambda} = 0$ should hold, from which refractive indices (n_\pm) are obtained. Substituting each of the refractive indices into the matrix-vector equation, one can obtain the associated polarization vectors ($\delta\mathbf{E}_\pm$).

In the configuration in Fig. 5, the parallel field condition $\mathbf{B}_0 = B_0\hat{z}$ and $\mathbf{E}_0 = E_0\hat{z}$ ($E_0 \geq 0$ and $B_0 > 0$) forces the permittivity and permeability tensors ϵ_E , ϵ_B , $\bar{\mu}_B$, and $\bar{\mu}_E$ in (27) to have the following structure:

$$\mathbf{r} = \begin{pmatrix} r & 0 & 0 \\ 0 & r & 0 \\ 0 & 0 & r + \tilde{r} \end{pmatrix}, \quad (37)$$

where r and \tilde{r} are given in Tab. V for each tensor. Furthermore, without loss of generality, the propagation vector can be assumed to be in the xz -plane: $\mathbf{k} = \omega n(\sin\theta, 0, \cos\theta)$. Then the matrix $\mathbf{\Lambda}$ becomes

$$\mathbf{\Lambda} = \begin{pmatrix} 1 - n^2 \cos^2 \theta & 0 & n^2 \sin \theta \cos \theta \\ 0 & 1 - n^2(1 + \mu \sin^2 \theta) & \epsilon_2 n \sin \theta \\ n^2 \sin \theta \cos \theta & \epsilon_2 n \sin \theta & 1 + \epsilon_1 - n^2 \sin^2 \theta \end{pmatrix}, \quad (38)$$

\mathbf{r}	r	\tilde{r}
ϵ_E	$\epsilon_E = 1 - \mathcal{L}_S^{(1)}$	$\tilde{\epsilon}_E = E_0^2 \mathcal{L}_{SS}^{(1)} + 2E_0 B_0 \mathcal{L}_{SA}^{(1)} + B_0^2 \mathcal{L}_{AA}^{(1)}$
ϵ_B	$\epsilon_B = -\mathcal{L}_A^{(1)}$	$\tilde{\epsilon}_B = -E_0 B_0 \mathcal{L}_{SS}^{(1)} + (E_0^2 - B_0^2) \mathcal{L}_{SA}^{(1)} + B_0 E_0 \mathcal{L}_{AA}^{(1)}$
$\bar{\mu}_B$	$\bar{\mu}_B = 1 - \mathcal{L}_S^{(1)}$	$\tilde{\bar{\mu}}_B = -B_0^2 \mathcal{L}_{SS}^{(1)} + 2E_0 B_0 \mathcal{L}_{SA}^{(1)} - E_0^2 \mathcal{L}_{AA}^{(1)}$
$\bar{\mu}_E$	$\bar{\mu}_E = \mathcal{L}_A^{(1)}$	$\tilde{\bar{\mu}}_E = E_0 B_0 \mathcal{L}_{SS}^{(1)} - (E_0^2 - B_0^2) \mathcal{L}_{SA}^{(1)} - B_0 E_0 \mathcal{L}_{AA}^{(1)}$

Table V. Components of the permittivity and permeability tensors for the configuration in Fig. 5. These tensors have the shape of (37).

where

$$\mu = \frac{\tilde{\mu}_B}{\epsilon_E}, \quad \epsilon_1 = \frac{\tilde{\epsilon}_E}{\epsilon_E}, \quad \epsilon_2 = \frac{\tilde{\epsilon}_B}{\epsilon_E}. \quad (39)$$

Below we assume $(\epsilon_1 + \mu + \epsilon_1\mu) < 0$ that held in all the cases we studied. When $(\epsilon_1 + \mu + \epsilon_1\mu) > 0$, the two modes denoted by the subscript \pm are swapped in the wrenchless case.

Solving the matrix equation is straightforward, but the general results are too lengthy to be presented. Instead, noting that ϵ_2 vanishes with E_0 (In Tab. V, $\mathcal{L}_{SA}^{(1)} = 0$ when $E_0 = 0$), we present only the expansions of the refractive indices and the polarization vectors up to $O(\epsilon_2^2)$ below. From $\det\mathbf{\Lambda} = 0$, the refractive indices are obtained:

$$n_+^2 \simeq \frac{1}{1 + \mu \sin^2 \theta} - \frac{(1 + \mu) \sin^2 \theta}{(\epsilon_1 + \mu + \epsilon_1\mu)(1 + \mu \sin^2 \theta)^2} \epsilon_2^2, \quad (40)$$

$$n_-^2 \simeq \frac{1 + \epsilon_1}{1 + \epsilon_1 \cos^2 \theta} + \frac{(1 + \epsilon_1) \sin^2 \theta}{(\epsilon_1 + \mu + \epsilon_1\mu)(1 + \epsilon_1 \cos^2 \theta)^2} \epsilon_2^2. \quad (41)$$

Then, the polarization vectors corresponding to n_{\pm}^2 are obtained by solving $\mathbf{\Lambda}_{\pm} \cdot \delta\mathbf{E}_{\pm} = 0$, where $\mathbf{\Lambda}_{\pm}$ is $\mathbf{\Lambda}$ (38) with $n^2 = n_{\pm}^2$. However, a blind application of the Gauss elimination fails to find the correct solution that becomes the wrenchless solution as ϵ_2 vanishes. By considering the limiting behavior of Λ_{ij} for $\epsilon_2 \rightarrow 0$ and requiring the solution's limiting behavior be consistent with that of Λ_{ij} , one can make $\mathbf{\Lambda}$, $\delta\mathbf{E}$, and $\mathbf{\Lambda} \cdot \delta\mathbf{E} = 0$ safely reduce those of the wrenchless case as $\epsilon_2 \rightarrow 0$. For example, as $\epsilon_2 \rightarrow 0$, $\Lambda_{+,22} \rightarrow \epsilon_2^2$, and $\Lambda_{+,23} \rightarrow \epsilon_2$, while other non-zero components do not vanish. Then, the solution of the type $(O(\epsilon_2), 1, O(\epsilon_2))^T$ yields the correct solution in terms of Λ_{ij} :

$$\delta\mathbf{E}_+ = \begin{pmatrix} \frac{\Lambda_{13}\Lambda_{23}}{\Lambda_{11}\Lambda_{33} - \Lambda_{13}^2} \\ 1 \\ -\frac{\Lambda_{11}\Lambda_{23}}{\Lambda_{11}\Lambda_{33} - \Lambda_{13}^2} \end{pmatrix}_{n^2=n_+^2} \simeq \begin{pmatrix} 0 \\ 1 \\ 0 \end{pmatrix} + \begin{pmatrix} \frac{1}{\epsilon_1 + \mu + \epsilon_1\mu} \frac{\cos \theta}{\sqrt{1 + \mu \sin^2 \theta}} \\ 0 \\ -\frac{1}{\epsilon_1 + \mu + \epsilon_1\mu} \frac{(1 + \mu) \sin \theta}{\sqrt{1 + \mu \sin^2 \theta}} \end{pmatrix} \epsilon_2, \quad (42)$$

where the denominator $\Lambda_{11}\Lambda_{33} - \Lambda_{13}^2$ does not vanish as $\epsilon_2 \rightarrow 0$. Similarly, as $\epsilon_2 \rightarrow 0$, $\Lambda_{-,23} \rightarrow \epsilon_2$, $\Lambda_{-,33} - \Lambda_{-,13}^2/\Lambda_{-,11} \rightarrow \epsilon_2^2$, while other non-zero components do not vanish. Then the solution of the type $(x, O(\epsilon_2), 1)^T$, where x is non-vanishing, yields the following solution:

$$\delta\mathbf{E}_- = \begin{pmatrix} -\frac{\Lambda_{13}}{\Lambda_{11}} \\ -\frac{\Lambda_{23}}{\Lambda_{22}} \\ 1 \end{pmatrix}_{n^2=n_-^2} \simeq \begin{pmatrix} -(1 + \epsilon_1) \cot \theta \\ 0 \\ 1 \end{pmatrix} + \begin{pmatrix} 0 \\ \frac{\sqrt{1 + \epsilon_1}}{\epsilon_1 + \mu + \epsilon_1\mu} \frac{\sqrt{1 + \epsilon_1} \cos^2 \theta}{\sin \theta} \\ 0 \end{pmatrix} \epsilon_2 + \begin{pmatrix} -\frac{(1 + \epsilon_1) \cot \theta}{\epsilon_1 + \mu + \epsilon_1\mu} \\ 0 \\ 0 \end{pmatrix} \epsilon_2^2, \quad (43)$$

where Λ_{11} and Λ_{22} do not vanish as $\epsilon_2 \rightarrow 0$.

In the wrenchless case, $E_0 = 0$ and, thus, $\epsilon_2 = 0$ hold. The corresponding refractive indices and polarization vectors are the zeroth-order terms in (40), (41), (41), and (43), which are consistent with those obtained by Melrose [4]. Unlike in the background-field-free vacuum, \mathbf{k} , $\delta\mathbf{E}_+$, and $\delta\mathbf{E}_-$ do not form an orthogonal triad in general, albeit $\mathbf{k} \perp \delta\mathbf{E}_+$ and $\delta\mathbf{E}_+ \perp \delta\mathbf{E}_-$. The polarization vector $\delta\mathbf{E}_+$ is along the y -axis, while $\delta\mathbf{E}_-$ lies in the xz -plane but not necessarily $\mathbf{k} \perp \delta\mathbf{E}_-$ [50]. An orthogonal triad is formed only when $\theta = \pi/2$: $\delta\mathbf{E}_-$ is aligned along the z -axis.

When $\theta = 0$, i.e., \mathbf{k} is along the z -axis, $n_{\pm}^2 = 1$ and $\delta\mathbf{E}_{\pm,z} = 0$ regardless of the wrench: the background field does not affect the propagation of the probe field because of the equal and opposite contributions from the virtual electrons and positrons.

The electromagnetic wrench, i.e., non-zero \tilde{b} , can significantly affect the vacuum birefringence, as shown in Fig. 6. In Fig. 6(a), the difference of the two refractive indices, $n_+ - n_-$, decreases noticeably for small \bar{a} as \tilde{b} increases: a 15% of reduction at $\bar{a} = 0.1$ for $\tilde{b} = 0.1$ ($B = B_{\text{cr}}$ and $E = E_{\text{cr}}$) albeit the reduction is negligible in the subcritical region. For $\tilde{b} = 0.2$, the reduction is about 50% in the supercritically magnetic region, in which pair production is not negligible for $\tilde{b} = 0.2$. In addition, the polarization vectors rotates due to the wrench, as shown in Fig. 6(b). When \mathbf{k} is along the x -axis ($\theta = \pi/2$), $\delta\mathbf{E}_+$ and $\delta\mathbf{E}_-$ on the yz -plane, and they are almost perpendicular to each other. In Fig. 6(b), $\delta\mathbf{E}_+$ rotates from the y -axis to the z -axis as \tilde{b} increases. The increase does not depend on \bar{a} until \tilde{b} reaches

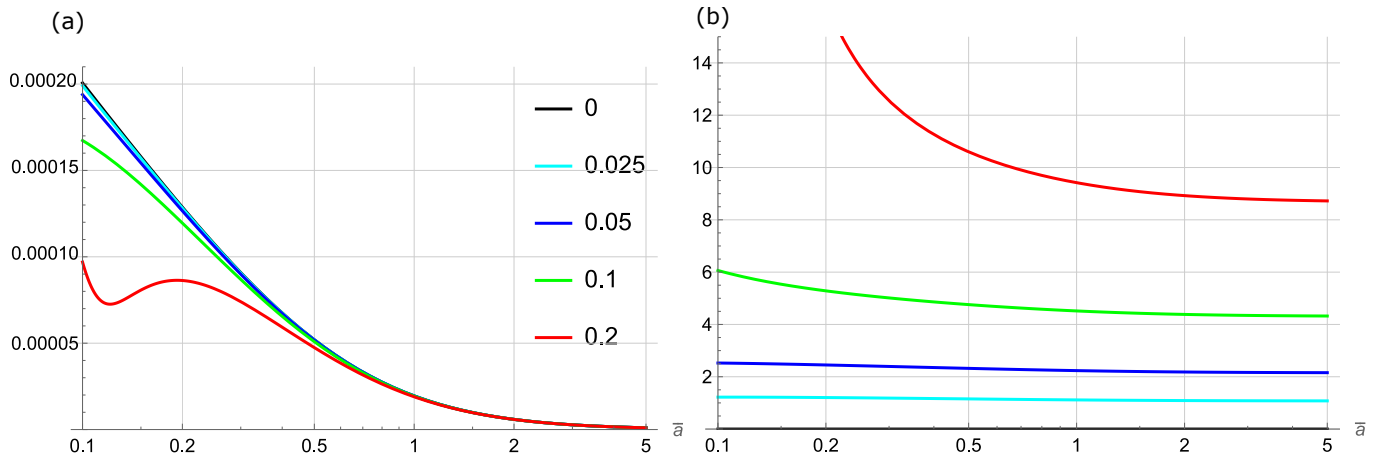


Figure 6. Effect of the electromagnetic wrench on vacuum birefringence: (a) $n_+ - n_-$ and (b) the angle (degree) of $\delta \mathbf{E}_+$ with respect to the y -axis for $\tilde{b} = 0, 0.025, 0.05, 0.1, 0.2$. The propagation vector \mathbf{k} of the probe field is along the x -axis ($\theta = \pi/2$).

0.1. For $\tilde{b} = 0.2$, the rotation angle is about 60 degrees at $\bar{a} = 0.1$. Even at lower values of \tilde{b} , the rotation angle amounts to a few degrees. In contrast, the wrenchless case allows no such rotation when $\theta = \pi/2$. Both the reduction of the differences of the refractive indices and the rotation of polarization vectors are new features of vacuum birefringence introduced by the non-zero electromagnetic wrench. These results suggest that the electromagnetic wrench should be taken into account in analyzing the vacuum birefringence when the electric field is a fraction of a supercritical magnetic field. Such a situation is anticipated in the magnetospheres of highly magnetized pulsars and neutron stars.

V. CONCLUSION

We have provided an explicit closed expression of the one-loop effective Lagrangian for the vacuum under an arbitrarily strong magnetic field superposed with a weaker electric field. To our knowledge, previous studies focused on the wrenchless case of $G = -\mathbf{E} \cdot \mathbf{B} = 0$. But our expression is valid for the cases of $G \neq 0$ as far as the pair production is not significant; in the case of significant pair production, a plasma of produced electron-positron pairs affects the vacuum polarization. Furthermore, the provided expressions, (13) and (14), is compact to facilitate theoretical analysis.

From the explicit closed expression, we have calculated the linear optical response of such vacuum to weak low-frequency fields. The permittivity and permeability tensors are given as (28), (29), (30), and (30) for an arbitrary one-loop effective Lagrangian. When the expansion form (14) of the Heisenberg–Euler and Schwinger effective Lagrangian is used, these tensors have values specified in Tabs. I, II, and III. The known results for the wrenchless and the weak-field cases in the literature are obtained by taking the limit of $b \rightarrow 0$ for arbitrary a and $a, b \rightarrow 0$ in our general expression, respectively.

With the permittivity and permeability tensors, we have worked out the modes of the probe field for the case where the background electric and magnetic fields are parallel to each other. The two refractive indices (40) and (41) clearly exhibits birefringence with the associated polarization vectors (42) and (43). Similarly, the results of the wrenchless case in the literature are the above limit of our expression. In the case with electromagnetic wrench, we have showed that electromagnetic wrench can reduce the difference of the refractive indices and rotate the polarization tensors; these effects have not been reported so far to our knowledge.

Our results can be used for the x-ray polarimetry of highly magnetized neutron stars. In the magnetosphere of such astrophysical objects, magnetic fields are comparable to or higher than the Schwinger field and accompanied by the induced weak electric fields. The electric field can noticeably change the polarimetric results, as shown in Fig. 6. For instance, when $B = 5B_{\text{cr}}$ and $E = 0.5E_{\text{cr}}$, the difference of the refractive indices are changed by 15%, and the polarization vectors rotate by 6° due to the non-negligible electric field along the magnetic field. At smaller values of E , the change is reduced but can grow to a significant level because the probe's propagation length is comparable to the size of the stars. Our expression that takes electromagnetic wrench into account enables an accurate analysis for such conditions.

ACKNOWLEDGMENTS

This work was supported by Institute for Basic Science (IBS) under IBS-R012-D1. The work of SPK was also supported by National Research Foundation of Korea (NRF) funded by the Ministry of Education (2019R1I1A3A01063183).

Appendix A: Numerical evaluation of the integral expression of $\mathcal{L}^{(1)}(a, b)$

We consider the numerical evaluation of the integral in (4). The integrand has a proper singularity at $z = 0$ with a well-defined limit (0) and thus poses no problem in principle. In numerical evaluation, however, the functional form in (5) leads to a serious loss of significant digits near $z = 0$. This problem can be avoided by using the Taylor expansion of the integrand around $z = 0$. More problematic are the poles of the $\cot(\tilde{b}z)$ at $z = n\pi/\tilde{b}$ ($n = 1, 2, \dots$). As we are interested only in the real part of $\mathcal{L}^{(1)}(a, b)$ to study vacuum birefringence, we take the principal value of the integral.

Taking into account of these problems, we split the integral into two parts, $I = I_1 + I_2$: one from 0 to z_b ($z_b \sim 0$ and $z_b \ll \pi/\tilde{b}$, the first pole) and the other from z_b to $(n + 1/2)\pi/\tilde{b}$, the midpoint between the n -th pole and $(n + 1)$ -th pole. As the number of poles increases, the numerical integration would converge to the exact value of the integral in (5). In the first part, we use the second-order Taylor expansion:

$$I_1(\bar{a}, \tilde{b}, n) = \int_0^{z_b} e^{-2\bar{a}z} \frac{z}{945} \left[21(1 + 5\tilde{b}^2 + \tilde{b}^4) + z^2(-2 - 7\tilde{b}^2 + 7\tilde{b}^4 + 2\tilde{b}^6) \right] dz. \quad (\text{A1})$$

The second part is given as

$$I_2(\bar{a}, \tilde{b}, n) = \text{Pr} \int_{z_b}^{\frac{(n+1/2)\pi}{\tilde{b}}} \frac{e^{-2\bar{a}z}}{z^3} \left[1 + \frac{z^2(1 - \tilde{b}^2)}{3} - \tilde{b}z^2 \coth(z) \cot(z\tilde{b}) \right] dz, \quad (\text{A2})$$

where Pr means the Cauchy principal value. To numerically evaluate the Cauchy principal value, we used Mathematica [51], which implements the algorithm presented in 2.12.8 of [52]. In the parameter range considered in our study, $z_b = 0.01$ and $n \leq 20$ gave a good convergence. A small number of poles are sufficient for convergence as a small value of \tilde{b} pushes the poles away from the origin, and the contribution from the region far from the origin is significantly suppressed by the factor $e^{-2\bar{a}z}/z^3$.

Appendix B: Analytic expression of $\mathcal{L}^{(1)}(a, 0)$

The integral expression of the one-loop effective action with $b = 0$ is obtained by taking the limit of $\tilde{b} = 0$ and using $\lim_{x \rightarrow 0} x \cot(x) = 1$ in (5):

$$\bar{\mathcal{L}}^{(1)}(a, 0) = \frac{m^4}{8\pi^2} \frac{1}{4\bar{a}^2} \int_0^\infty \frac{e^{-2\bar{a}z}}{z^3} \left[1 + \frac{z^2}{3} - z \coth(z) \right] dz, \quad (\text{B1})$$

where $\bar{a} = m^2/(2ea)$. The integration can be performed by expanding $z \coth z$ is expanded around $z = 0$:

$$z \coth z = \sum_{n=0}^{\infty} \frac{B_{2n}(2z)^{2n}}{(2n)!}, \quad (\text{B2})$$

where B_{2n} are the Bernoulli numbers. This expansion is convergent for $|z| < \pi$, as can be seen by the root test. However, it can be substituted into (B1) to yield an asymptotic expression for $\bar{a} \rightarrow \infty$ because $\exp(-2\bar{a}z)$ suppresses the contribution from the region of $z \gg 1/(2a)$ if the remaining part of the integrand has a polynomial divergence at most. By using the formula $\int_0^\infty e^{-\alpha z} z^p dz = \Gamma(p+1)/\alpha^{p+1}$, we can obtain an asymptotic expression of $\mathcal{L}^{(1)}(a, 0)$:

$$\bar{\mathcal{L}}^{(1)}(a, 0) \sim -\frac{m^4}{8\pi^2} \sum_{n=2}^{\infty} \frac{B_{2n}}{2n(2n-1)(2n-2)} \frac{1}{\bar{a}^{2n}}. \quad (\text{B3})$$

This series (B3) is divergent for any finite value of \bar{a} , which can be found by the root test, and, as $\bar{a} \rightarrow \infty$, it is asymptotic to a function involving the Hurwitz zeta function $\zeta(s, \bar{a})$ (25.11.44 in [35]):

$$-\sum_{n=2}^{\infty} \frac{B_{2n}}{2n(2n-1)(2n-2)} \frac{1}{\bar{a}^{2n-2}} \sim H(\bar{a}) = \zeta'(-1, \bar{a}) - \frac{1}{12} + \frac{\bar{a}^2}{4} - \left(\frac{1}{12} - \frac{\bar{a}}{2} + \frac{\bar{a}^2}{2} \right) \ln \bar{a}, \quad (\text{B4})$$

where $\zeta'(-1, \bar{a}) = d\zeta(s, \bar{a})/ds|_{s=-1}$. Consequently,

$$\bar{\mathcal{L}}^{(1)}(\bar{a}, 0) \sim \frac{m^4}{8\pi^2} \frac{H(\bar{a})}{\bar{a}^2}. \quad (\text{B5})$$

Remarkably, this asymptotic relation turns out to be equality. The formula (B5) is exactly the expression of $\bar{\mathcal{L}}^{(1)}(\bar{a}, 0)$ obtained either by the dimensional regularization of (B1) [25, 26] or by the Schwinger-DeWitt in-out formalism with Γ -function regularization [27].

We mention a useful symmetry of the effective Lagrangian. From (2), F and $|G|$ are invariant when a (b) is replaced by ib ($-ia$), leading to a symmetry relation:

$$\mathcal{L}(a, b) = \mathcal{L}(ib, -ia). \quad (\text{B6})$$

Therefore, when the expression of $\mathcal{L}(a, 0)$ is available, setting $a = ib'$ yields the expression of $\mathcal{L}(0, b')$:

$$\mathcal{L}(a, 0) = \mathcal{L}(ib', 0) = \mathcal{L}(0, -i(ib')) = \mathcal{L}(0, b') = \frac{m^4}{8\pi^2} \frac{1}{b'^2} \left[\frac{\pi}{4\alpha} - H(-ib') \right], \quad (\text{B7})$$

which matches the one-loop effective Lagrangian in a uniform electric field. Further, note that the imaginary part of (B7) is equivalent to the sum of the residues from the simple poles of (4), which was explicitly shown in [27].

Appendix C: Expression of $H^{(2n)}(z)$

The even-order derivatives of $H(z)$ can be explicitly obtained. The function $H(z)$ consists of two parts:

$$H(z) = \zeta'(-1, z) + h(z) = \zeta'(-1, z) - \frac{1}{12} + \frac{z^2}{4} - \left(\frac{1}{12} - \frac{z}{2} + \frac{z^2}{2} \right) \ln z, \quad (\text{C1})$$

where $\zeta'(-1, z) = d\zeta(s, z)/ds|_{s=-1}$. The function $\zeta(s, z)$ is the Hurwitz zeta function, defined as (25.11.1 in [35]):

$$\zeta(s, z) = \sum_{n=0}^{\infty} \frac{1}{(n+z)^s} \quad (\text{Re}\{s\} > 1, z \neq 0, -1, -2, \dots).$$

As far as $s \neq 1$, the expression can be analytically continued. To calculate $\partial_z^{2n} \zeta'(-1, z)$, we begin with the following identity (25.11.17 in [35]):

$$\partial_z \zeta(s, z) = -s \zeta(s+1, z), \quad (s \neq 0, 1 \text{ and } \text{Re}\{z\} > 0). \quad (\text{C2})$$

Differentiating with respect to s and setting $s = -1$, we obtain

$$\partial_z \zeta'(-1, z) = -\zeta(0, z) + \zeta'(0, z) = z - \frac{1}{2} + \ln \Gamma(z) - \frac{1}{2} \ln(2\pi), \quad (\text{C3})$$

where $\zeta(0, z) = -z + 1/2$ and $\zeta'(0, z) = \ln \Gamma(z) - \ln(2\pi)/2$ are used for the second equality (25.11.13 and 25.11.18 in [35]). Differentiating with respect to z successively and using the definition of the polygamma function (5.2.2 and 5.15 in [35])

$$\psi^{(m)}(z) = d^{m+1}(\ln \Gamma(z)) / dz^{m+1}, \quad (\text{C4})$$

we obtain the formula of $\partial_z^{2n} \zeta'(-1, z)$:

$$\partial_z^{2n} \zeta'(-1, z) = \delta_{n1} + \psi^{(2n-2)}(z), \quad n \geq 1. \quad (\text{C5})$$

The successive differentiation of $h(z)$ in (C1) is straightforward, and, consequently, the formula of $H^{(2n)}(z)$ is given as

$$H^{(2n)}(z) = \psi^{(2n-2)}(z) + \frac{1}{12} \frac{\Gamma(2n)}{z^{2n}} + \frac{1}{2} \frac{\Gamma(2n-1)}{z^{2n-1}} + \frac{\Gamma(2n-2)}{z^{2n-2}} \theta(n-2) - \delta_{n1} \ln z, \quad (n \geq 1), \quad (\text{C6})$$

where $\theta(n)$ is the unit step function with $\theta(n \geq 0) = 1$.

- [1] W. Heisenberg and H. Euler, *Zeitschr. Phys* **98**, 714 (1936).
- [2] V. F. Weisskopf, *Dan. Mat. Fys. Medd.* **14**, 1 (1936).
- [3] J. Schwinger, *Phys. Rev.* **82**, 664 (1951).
- [4] D. B. Melrose, *Quantum plasmadynamics: magnetized plasmas*, Lecture notes in physics No. v. 854 (Springer, New York, 2013).
- [5] J. W. Yoon, Y. G. Kim, I. W. Choi, J. H. Sung, H. W. Lee, S. K. Lee, and C. H. Nam, *Optica* **8**, 630 (2021).
- [6] C. N. Danson, C. Haefner, J. Bromage, T. Butcher, J.-C. F. Chanteloup, E. A. Chowdhury, A. Galvanauskas, L. A. Gizzi, J. Hein, D. I. Hillier, and et al., *High Power Laser Sci. Eng.* **7**, e54 (2019).
- [7] R. Moreh and S. Kahana, *Phys. Lett. B* **47**, 351 (1973).
- [8] P. Rullhusen, U. Zurmühl, F. Smend, M. Schumacher, H. G. Börner, and S. A. Kerr, *Phys. Rev. C* **27**, 559 (1983).
- [9] G. Jarlskog, L. Jönsson, S. Prünster, H. D. Schulz, H. J. Willutzki, and G. G. Winter, *Phys. Rev. D* **8**, 3813 (1973).
- [10] D. d'Enterria and G. G. da Silveira, *Phys. Rev. Lett.* **111**, 080405 (2013), [Erratum: *Phys.Rev.Lett.* **116**, 129901 (2016)], arXiv:1305.7142 [hep-ph].
- [11] ATLAS Collaboration, *Nature Phys.* **13**, 852 (2017).
- [12] A. M. Sirunyan *et al.* (CMS), *Phys. Lett. B* **797**, 134826 (2019), arXiv:1810.04602 [hep-ex].
- [13] F. Della Valle, A. Ejlli, U. Gastaldi, G. Messineo, E. Milotti, R. Pengo, G. Ruoso, and G. Zavattini, *Eur. Phys. J. C* **76**, 24 (2016), arXiv:1510.08052 [physics.optics].
- [14] F. Karbstein, C. Sundqvist, K. S. Schulze, I. Uschmann, H. Gies, and G. G. Paulus, *New J. Phys.* **23**, 095001 (2021).
- [15] B. Shen, Z. Bu, J. Xu, T. Xu, L. Ji, R. Li, and Z. Xu, *Plasma Phys. Control. Fusion* **60**, 044002 (2018).
- [16] C. Pellegrini, *Phys. Scr.* **T169**, 014004 (2016).
- [17] A. T. Schmitt, Y. Joly, K. S. Schulze, B. Marx-Glowna, I. Uschmann, B. Grabiger, H. Bernhardt, R. Loetzsch, A. Juhin, J. Debray, H.-C. Wille, H. Yavaş, G. G. Paulus, and R. Röhlsberger, *Optica* **8**, 56 (2021).
- [18] G. Vasisht and E. Gotthelf, *Astrophys. J. Lett.* **486**, L129 (1997).
- [19] S. A. Olausen and V. M. Kaspi, *ApJS* **212**, 6 (2014).
- [20] V. M. Kaspi and A. M. Beloborodov, *Annu. Rev. Astron. Astrophys.* **55**, 261 (2017).
- [21] P. Goldreich and W. H. Julian, *Astrophys. J.* **157**, 869 (1969).
- [22] T. Enoto, S. Kisaka, and S. Shibata, *Rep. Prog. Phys.* **82**, 106901 (2019).
- [23] A. Santangelo, S. Zane, H. Feng, R. Xu, V. Doroshenko, E. Bozzo, I. Caiazzo, F. C. Zelati, P. Esposito, D. Gonzalez-Caniulef, and others, *SCIENCE CHINA Physics, Mechanics & Astronomy* **62**, 1 (2019).
- [24] Z. Wadiasingh, G. Younes, M. G. Baring, A. K. Harding, P. L. Gonthier, K. Hu, A. v. d. Horst, S. Zane, C. Kouveliotou, A. M. Beloborodov, C. Prescod-Weinstein, T. Chattopadhyay, S. Chandra, C. Kalapotharakos, K. Parfrey, and D. Kazanas, *Bulletin of the AAS* **51** (2019).
- [25] W. Dittrich, *J. Phys. A: Math Gen.* **9**, 1171 (1976).
- [26] W. Dittrich, W.-y. Tsai, and K.-H. Zimmermann, *Phys. Rev. D* **19**, 2929 (1979).
- [27] S. P. Kim and H. K. Lee, *J. Korean Phys. Soc.* **74**, 930 (2019).
- [28] C. M. Kim and S. P. Kim, *Magnetars as laboratories for strong field qed* (2021), arXiv:2112.02460 [astro-ph.HE].
- [29] W. Dittrich and H. Gies, *Probing the quantum vacuum: perturbative effective action approach in quantum electrodynamics and its application*, Springer tracts in modern physics No. v. 166 (Springer, Berlin ; New York, 2000).
- [30] J. D. Jackson, *Classical electrodynamics*, 3rd ed. (Wiley, New York, 1999).
- [31] M. D. Schwartz, *Quantum field theory and the standard model* (Cambridge University Press, New York, 2014).
- [32] V. I. Ritus, *Sov. Phys. JETP* **42**, 774 (1976).
- [33] H. Gies and F. Karbstein, *J. High Energy Phys.* **2017**, 108.
- [34] F. Karbstein, *Phys. Rev. Lett.* **122**, 211602 (2019), arXiv:1903.06998 [hep-th].

- [35] F. W. J. Olver, *NIST Handbook of Mathematical Functions*, 1st ed. (Cambridge University Press, Cambridge ; New York, 2010).
- [36] J. S. Heyl and L. Hernquist, *Phys. Rev. D* **55**, 2449 (1997).
- [37] Y. M. Cho and D. G. Pak, *Phys. Rev. Lett.* **86**, 1947 (2001).
- [38] U. D. Jentschura, H. Gies, S. R. Valluri, D. R. Lamm, and E. J. Weniger, *Can. J. Phys.* **80**, 267 (2002).
- [39] Y. M. Cho, D. G. Pak, and M. L. Walker, *Phys. Rev. D* **73**, 065014 (2006).
- [40] M. Born, E. Wolf, A. B. Bhatia, P. C. Clemmow, D. Gabor, A. R. Stokes, A. M. Taylor, P. A. Wayman, and W. L. Wilcock, *Principles of Optics: Electromagnetic Theory of Propagation, Interference and Diffraction of Light*, 7th ed. (Cambridge University Press, 1999).
- [41] V. B. Berestetskii, L. P. Pitaevskii, and E. M. Lifshitz, *Quantum Electrodynamics: Volume 4*, 2nd ed. (Butterworth-Heinemann, Oxford, 1982).
- [42] Z. Bialynicka-Birula and I. Bialynicki-Birula, *Phys. Rev. D* **2**, 2341 (1970).
- [43] F. Karbstein and R. Shaisultanov, *Phys. Rev. D* **91**, 085027 (2015), arXiv:1503.00532 [hep-ph].
- [44] J. Mckenna and P. M. Platzman, *Phys. Rev.* **129**, 2354 (1963).
- [45] S. L. Adler, *Ann. Phys.* **67**, 599 (1971).
- [46] D. B. Melrose and R. C. McPhedran, *Electromagnetic Processes in Dispersive Media*, 1st ed. (Cambridge University Press, 1991).
- [47] M. Fiebig, *J. Phys. D: Appl. Phys.* **38**, R123 (2005).
- [48] W. Eerenstein, N. D. Mathur, and J. F. Scott, *Nature* **442**, 759 (2006).
- [49] T. H. O'Dell, *Philos. Mag.* **7**, 1653 (1962).
- [50] S.-W. Hu and B.-B. Liu, *J. Phys. A: Math Theor.* **40**, 13859 (2007).
- [51] W. R. Inc., *Mathematica*, Version 13.0.0, Champaign, IL, 2021.
- [52] P. Davis, P. Rabinowitz, and W. Rheinboldt, *Methods of Numerical Integration*, Computer Science and Applied Mathematics (Elsevier Science, 2014).